Alma Mater Studiorum Università di Bologna
Archivio istituzionale della ricerca

A 3D optimization algorithm for sustainable cutting of slabs from ornamental stone blocks

(Article begins on next page)

19 October 2024

1 **Abstract**

2 Ornamental stones are natural building materials, extracted from quarries, which need to be cut

3 and processed sustainably. Natural discontinuities adversely affect the sawing/cutting of blocks

4 into commercial-size slabs. This work presents a 3D optimization algorithm for the sawing/cutting

5 of ornamental stone blocks. The developed algorithm is based on 3D modeling of discontinuities

6 as data input. The algorithm search for the intersection between a 3D cutting grid formed of a

7 determined size of slabs and the model of discontinuities leading to calculate the recovery ratio

8 considering several cutting orientations and displacements of the 3D cutting grid. The algorithm

9 was coded in a program named SlabCutOpt that allows speed problem solving. SlabCutOpt was

10 implemented on a real case study of a commercial-size limestone block extracted from a quarry

11 in Italy. A number of 37 different commercial-sizes of slabs forming 37 cutting grids were tested

12 to investigate the optimum results in geo-environmental direction (recovery ratio) and economic

13 directions (revenue). The findings revealed that a certain slab size gave the optimum recovery

14 ratio, whilst another slab size provided the optimum revenue.

15 **Keywords:**

18 **1. Introduction**

19 Ornamental stones are natural non-renewable resources that have to be exploited and processed

20 in an optimized way to minimize waste production and maximize revenue. It is just a third of the

21 extracted stone raw material arrives to the global market as a finished product, whilst the two-

22 thirds remaining are waste, considering the worldwide average in the ornamental stones

23 extraction [1]. Ornamental stones are considered as main economic resources for many countries

24 overall the world [2]. Therefore, and since ornamental stones are natural non-renewable

25 resources, they have to be extracted and processed sustainably for environmental and economic

26 reasons.

27 The right exploitation of ornamental stone is crucial for any competitive economic growth

28 roadmaps of countries aiming the sustainable development [3]. Environmental and economic

29 sustainability strategies for ornamental stone industry is being studied in literature [4–7]. There

30 are recent trends for stone waste recycling [8–11], but minimization of waste production during

31 exploitation and processing is with more preferable impact environmentally and economically.

32 Ornamental stones blocks are extracted from quarries. Blocks are cut to obtain slabs and tiles.

33 The size of tiles and slabs depends on building and construction final applications. Slabs and tiles

34 can be subjected to several types of surface treatment. From a commercial point of view, the

35 main factor that define the commercial price is the dimension of slabs. In General, the larger the

36 size of slabs, the selling price is higher.

37 Blocks are cut/sawed in processing plants using diamond disc saws, diamond blade saws, or gang-

38 saws. Currently, the most used is multi-blades gang-saws that can cut a block to slabs with certain

39 and specific thickness. Several previous work studied the cutting process of ornamental stones

40 considering the sawability [12], the cutting energy consumption [13], and the sawing

41 performance [14]. In this paper, we consider a further aspect that is needed to fulfil the

42 sustainable development of the cutting/sawing process of ornamental stone blocks.

43 Discontinuities, fractures and bedding planes define the exploitability of commercial-size

44 ornamental stone blocks from quarries [15]. Discontinuities not detected on the outcrops

45 adversely affect the quality of ornamental stone blocks. The recovery ratio of the stone deposit

46 depends strongly on these parameters. The possibility to detect structural weaknesses regions

47 of ornamental stone blocks before cutting it is an environmental and economic important phase.

48 The most common methods used in practice are the traditional observation based methods,

49 which can lead to erroneous or non-reliable results. Nowadays, there is an unsatisfactory lack in

50 the use of non-destructive methods for fracture detection in ornamental stone blocks.

51 A survey on fracture detection methods is provided in [16]. Among the used methods, the Ground

52 Penetrating Radar (GPR), appeared to be a valid non-destructive method for discontinuities

53 detection in ornamental stone quarries of different rock types [17–28].

54 With reference to the use of GPR in order to detect and model discontinuities and assessing of

55 rock blocks, it worth to mention the works in [24,29–33]. However, in [32], it is possible to analyze

56 the application of a 3D deterministic discontinuities model, to ornamental stone blocks,

57 significant for the topic of this paper.

58 Previous works presented stochastic or geometric algorithms, aiming to analyze the fracture

59 geometry and quantify the volume of the so called natural blocks, that are defined by the natural

60 discontinuities planes [34–36]. The natural rock blocks geometry identification can be used for a

61 preliminary reserves estimation in quarries, as in the case of the calculation of the maximum

62 largest cuboid [37] or of the marketable block size [38] that fit into the natural rock blocks. The

63 previously listed methods were based on the manual survey method of out-cropping

64   discontinuities. The target of this paper can be achievable when hidden discontinuities can be

65   detected and modeled as well. Identification of natural blocks and the maximum largest cuboid

66   algorithms may not work well on the ornamental stone blocks scale, considering that on that

67   scale planes of discontinuities may or mayn't be intersected at this small scale.

68   A number of works have considered the production optimization at quarry or bench scale [39–

69   42], based on the mapping of fractures through the manual survey method. However, this paper

70   considers the production optimization at a block scale through a new methodological approach,

71   on the basis of a 3D deterministic modeling approach-based GPR that models fractures as 3D

72   surfaces, not planes as typically modeled in literature. The method presented in this paper does

73   not have a limitation to the number of fracture families and their restricted input parameters

74   (dip angle and dip direction, spacing). It is worth mentioning the work of [43] that provided a

75   geometrical design computation of optimum cutting shapes from polygonal boundary

76   ornamental stone slabs.

77   Several open questions on production optimization during the cutting phase of slabs from a block

78   are: (i) which dimensions of slabs/tiles to be cut? (ii) Which is the best orientation of block cutting

79   (parallel to x-plane, y-plane, or z-plane)? and (iii) What is the optimum angle of slabs cut from a

80   block? In order to answer these questions, this paper presents a 3D computational algorithm

81   developed to optimize the cutting grid pattern of a block, starting from a 3D fracture modeling

82   method presented in [17]. The developed algorithm was coded using the C++ programming

83   language in a software package named SlabCutOpt. The software code SlabCutOpt allows the

84   computation of the problem and the visualization of the results. Indeed, the latter atomizes the

85   finding of the optimum design related to the cutting grid pattern of a block for each commercial

86   slab size tested, providing the optimum recovery ratio. The paper presents the application of the

87   SlabCutOpt code to a case study of a limestone block and discusses the optimization results. To

88   the best of the authors' knowledge, this is the first attempt of a production optimization model

89   at the block scale.

90   **2. Method**

91   **2.1. The optimization algorithm**

92   The developed 3D optimization algorithm generates a 3D cutting grid for a block. The 3D cutting

93   grid represents the slabs with equal dimensions (dim_x, dim_y, dim_z), as shown in Fig. 1. The

94   3D cutting grid was built starting from the center of the block (C) with a specified number of cuts

95   in three orthogonal directions: n_x, n_y, n_z. The specified dimensions cover the 3D domain of the

96   block, during the whole run of the algorithm, using a number of slabs in a way that n_i *dim__>

97   block dimension I, with i=x,y,z.. The block is described by the minimum and maximum Cartesian

98   coordinates (x_min, x_max, y_min, y_max, and z_min: z_max).

99
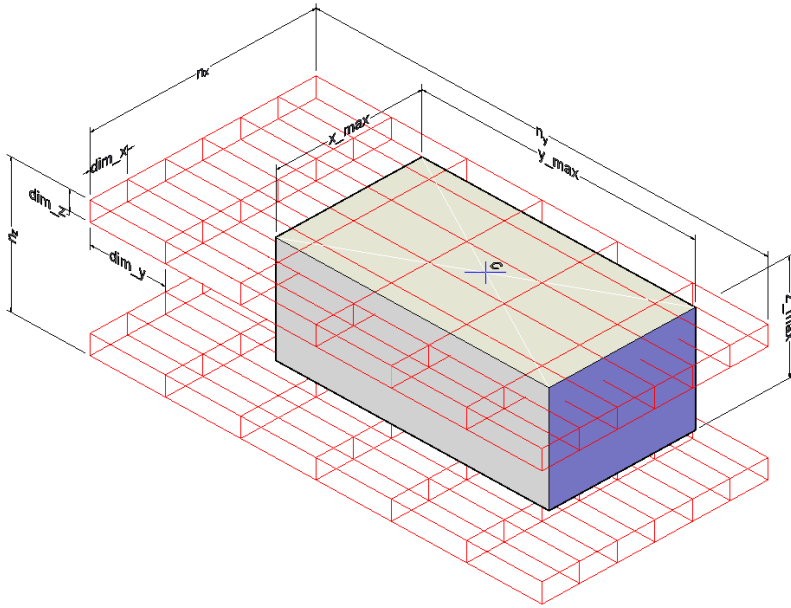
Fig. 1. Illustrative sketch showing the 3D cutting grid of the slabs (colored in red) within the block body.

The algorithm detects the intersection between the slabs (cutting grid) and the fractures model or the six faces of the block body. In this paper, the discontinuities model represents a model of fractures, joints, and voids. Iteratively, the cutting grid is rotated using a 3D rotation mode. The cutting orientations of the slabs can be parallel to the XY plane, XZ plane, or YZ plane of the block (see Fig. 2 and Table 1). The cutting grid is also subjected to several 3D displacements (dx, dy, dz), defined by Eq. (1), Eq. (2), and Eq. (3).

$$(-dim\_x)/2 \leq dx < (+dim\_x)/2, \text{ with a step of } dx\_step, \text{ for } dx \tag{1}$$

$$(-dim\_y)/2 \leq dy < (+dim\_y)/2, \text{ with a step of } dy\_step, \text{ for } dy \tag{2}$$

Commentato [SB1]: I addes plural. Is correct?

110   (-dim_z)/2 ≤ dz < (+dim_z)/2, with a step of dz_step, for dz   (3)
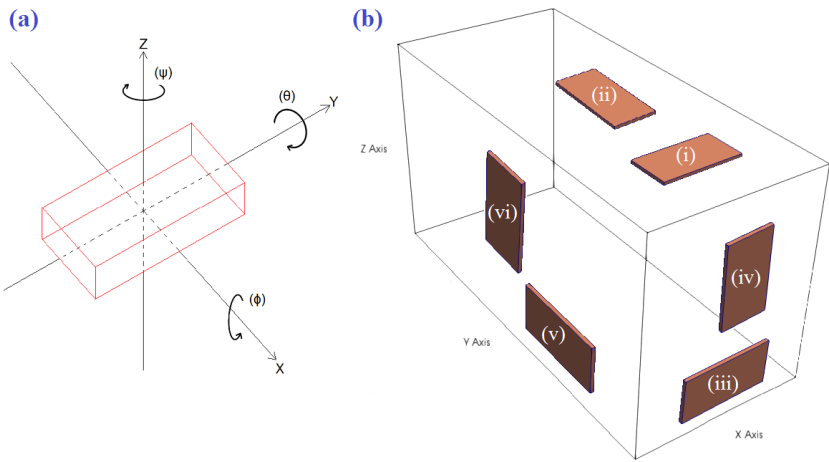
111

112   Fig. 2. (a) The possible orientation-rotation angles of the 3D cutting grid of the slabs; (b) A sketch

113   showing the possible orientation-rotations within a block (details of the sub-figures numbering

114   are given in Table 1).

115   **Table 1**
116   The possible orientations-rotations of the cutting grid.

cutting orientation of slabs	rotation of slabs	the relative orientation-rotation			figure
		theta θ	phi φ	psi ψ	
XY plane	0.0°	0.0°	0.0°	0.0°	Fig. 2b(i)
XY plane	90.0°	0.0°	0.0°	90.0°	Fig. 2b(ii)
XZ plane	0.0°	90.0°	0.0°	0.0°	Fig. 2b(iii)
XZ plane	90.0°	90.0°	90.0°	0.0°	Fig. 2b(iv)
YZ plane	0.0°	90.0°	0.0°	90.0°	Fig. 2b(v)
YZ plane	90.0°	90.0°	90.0°	90.0°	Fig. 2b(vi)

117
118
119   The intersection between a slab and a discontinuity (or with the faces of the block body) is

120   detected by using a segment/triangle intersection algorithm [44]. The segment/triangle

121   intersection algorithm [44] compute the signs of 4 determinants and don't require any explicit

122 constructions that can be subject to numerical errors. Each discontinuity and the faces of the

123 block body are geometrically defined by 3D triangles. For each 3D cutting grid patterns, each slab

124 is checked if it intersects a discontinuity or a face of the block. This implies that a slab that is

125 composed by 12 edge segments, the algorithm checks the intersection between the 12 edge

126 segments and all the triangles that represent the discontinuities model. The algorithm computes

127 the number of non-intersected slabs and total number of slabs (intersected + non-intersected)

128 within the block body. The recovery ratio is calculated for each displacement and for each

129 orientation-rotation to determine the optimum cutting grid pattern using Eq. (4). The recovery

130 ratio is also called coefficient of utilization as given and defined in [45]. The recovery ratio

131 described in Eq. (4) is limited to a fixed slab size as defined by the user. The SlabCutOpt algorithm

132 consider a regular cutting grid, because the use of several slab sizes at the same time (irregular

133 cutting grid), can theoretically provide higher recovery ratio, but a grid of several different sizes

134 of slabs cut from a block can be hardly/practically carried out within the typical cutting process

135 of ornamental stone blocks. Considering also that small non-commercial sizes of slabs may be

136 included in the cutting grids. In most cases, the quarrymen cut a block to produce a specific size

137 of slabs which the markets already need. However, in this paper, we aimed at comparing the

138 results of several cutting grids comparing several slab size.

139 $$recovery\ (\%) = \frac{volume\ of\ non-intersected\ slabs\ with\ full\ dimension\ inside\ the\ block\ body\ x\ 100}{total\ volume\ of\ the\ block\ body} \quad (4)$$

140 In the processing plants, the cutting saws work with a continuous water flow that is required for

141 cooling and reducing the dust emissions caused by sawing. The dust is the material lost during

142 sawing which can be then reused for further applications [46–49]. The algorithm presented in

143   this paper takes into account the thickness of the cutting saw and the volume of material

144   lost/wasted due to sawing.

145   **2.2. Software development**

146   The developed algorithm was coded using the C++ programming language and makes use of the

147   OpenMP library for multithreading computations. The software package developed was named

148   "SlabCutOpt" on the basis of the algorithm aim: Slab Cutting Optimization.

149   **2.2.1. Input data files**

150   The input data of SlabCutOpt is composed of several files:

151   • SlabCutOpt.par: ASCII file containing the input parameters of cutting grid. It has to contain the

152   geometric dimensions of the block body, the parameters about orientation-rotation and

153   displacement and options concerning the operating mode and the output mode, etc. The

154   algorithm can also work only in 2D, avoiding testing for the Z direction. See Appendix A for details;

155   • PLY files: each discontinuity or set of discontinuities has to modelled in one or more file using

156   the polygon file format (ply) [50]. See Appendix B for details;

157   • PLY_FileList.dat: this is the ASCII file with the list of the ply files. See Appendix C for details.

158   • slab_dimensions.dat: this is the ASCII file contains the list of the several sizes of slabs to be

159   tested. See Appendix D for details.

160

161

2.2.2. Files of results

The results files of SlabCutOpt are ASCII files with detailed information on the computations of the grid cutting optimization search, in addition to files needed for the 3D visualization. The results files of SlabCutOpt are:

•Results.log file: this is an ASCII file, where each row contains, for each slab size, the orientation of the 3D cutting grid, the applied displacements, the number of non-intersected slabs inside the block body, and the number of intersected slabs inside the block body. See Appendix E for details.

•slabs vtu files: optionally, a set of vtu files are generated for the 3D visualization of the cutting grid. The vtu file generation can be the whole set of cutting grids scenarios or just for the best solution (maximum number of non-intersected slabs). A slab type code is assigned to each slab, in the vtu files, to allow an easy visual perception of the kind of slab: out bounding of the block, intersected and non-intersected slabs. The vtu files can be then visualized using, for example, the free and open source visualization software ParaView [51]. Fig. 3 shows a schematic diagram of the software package structure.

182

192 **3. Case study**

193 SlabCutOpt was applied to a real case study. The rock type of the commercial size block under

194 study (1.55 m x 2.9 m x 1.10 m) was compacted limestone with a creamy-white color. It is a highly

195 fractured limestone block whose out-cropping fractures and furthermore discontinuities could

196 be detected and deterministically modeled as 3D surfaces based on GPR survey, this model of

197 discontinuities and description of the block under study is presented in [32].

198 The revenue estimation of the block was carried out on the basis of a Relative Money Value (RMV)

199 for each slab size, calculated by Eq. (5) (given that the real selling prices are confidential):

200 RMV for a slab = the slab selling price (€) / the maximum unit price of all the slabs (€)   (5)

201   Table 2 presents the selected commercial sizes of the slabs with their RMV and surface area. A

202   quasi linear correlation between the size (area) of the slabs and the commercial price was clearly

203   found (Figure 4). The optimization solutions were investigated by SlabCutOpt for the whole

204   commercial-sizes of the slabs listed in Table 2.

205

206

207

208

209

210

211

212

213

214

215

216

217   **Table 2**
218   The RMV of the commercial-sizes of slabs tested.

| size No.	dimensions of slabs and tiles			RMV per unit	surface area (m²)
	x (cm)	y (cm)	z (cm)		
size 1	40.00	20.00	1.50	0.082	0.08
size 2	50.00	25.00	1.50	0.127	0.13
size 3	40.00	20.00	2.00	0.087	0.08
size 4	50.00	25.00	2.00	0.136	0.13
size 5	60.00	30.00	1.50	0.207	0.18
size 6	30.00	30.00	1.50	0.104	0.09
size 7	40.00	40.00	1.50	0.184	0.16
size 8	60.00	45.00	1.50	0.311	0.27
size 9	45.00	45.00	1.50	0.233	0.20
size 10	48.00	48.00	1.50	0.265	0.23
size 11	60.00	30.00	2.00	0.219	0.18
size 12	30.00	30.00	2.00	0.110	0.09
size 13	40.00	40.00	2.00	0.195	0.16
size 14	60.00	45.00	2.00	0.329	0.27
size 15	45.00	45.00	2.00	0.246	0.20
size 16	48.00	48.00	2.00	0.280	0.23
size 17	80.00	40.00	1.50	0.442	0.32
size 18	80.00	48.00	1.50	0.531	0.38
size 19	80.00	40.00	2.00	0.463	0.32
size 20	80.00	48.00	2.00	0.556	0.38
size 21	30.50	30.50	1.00	0.107	0.09
size 22	30.00	15.00	3.00	0.040	0.05
size 23	30.00	10.00	3.00	0.027	0.03
size 24	30.00	110.00	2.00	0.380	0.33
size 25	35.00	150.00	2.00	0.604	0.53
size 26	40.00	190.00	2.00	0.875	0.76
size 27	30.00	110.00	3.00	0.434	0.33
size 28	35.00	150.00	3.00	0.691	0.53
size 29	40.00	190.00	3.00	1.000	0.76
size 30	15.00	60.00	2.00	0.098	0.09
size 31	20.00	80.00	2.00	0.174	0.16
size 32	25.00	100.00	2.00	0.271	0.25
size 33	25.00	125.00	2.00	0.339	0.31
size 34	15.00	60.00	3.00	0.104	0.09
size 35	20.00	80.00	3.00	0.184	0.16
size 36	25.00	100.00	3.00	0.288	0.25
size 37	25.00	125.00	3.00	0.360	0.31
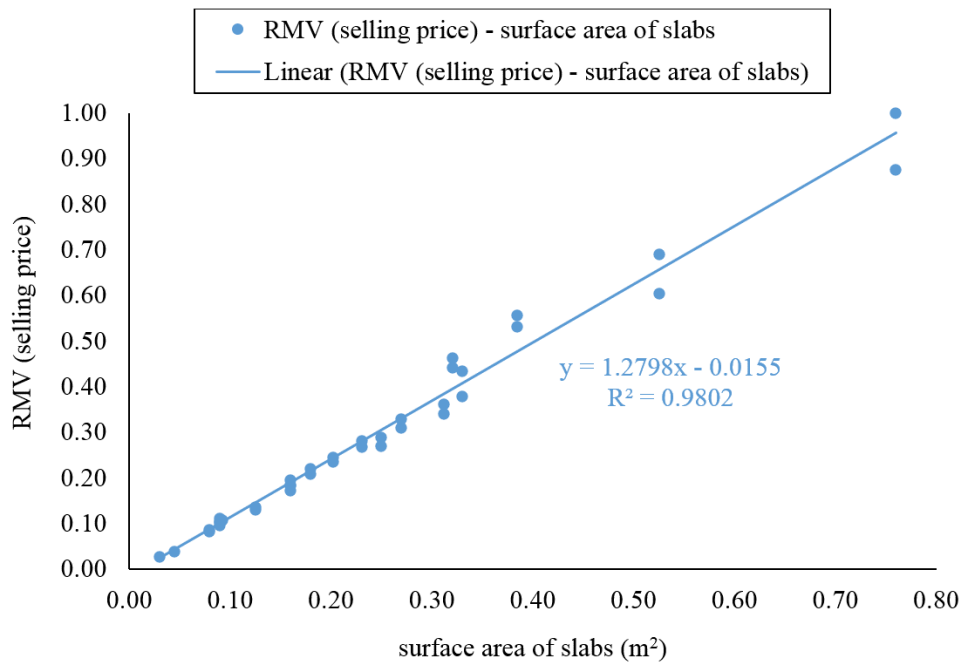
Fig. 4. Correlation between the sizes of the slabs and the RMV.

4. Results

For each slab size of Table 2, a 3D cutting grid was used to compute the non-intersected slabs, using the six orientations-rotations and several displacements of the cutting grid. The algorithm parameters used in this study (SlabCutOpt.par file) are presented in Appendix A. Fig. 5 shows, for slab size No. 1 of Table 2, the computation results of several simulated 3D cutting grids. For clarity, the discontinuities inside the limestone block body are represented using the same colors as in the model presented in [32]. The cutting saw thickness is clearly visible in Fig. 5g and Fig 5h, as the slabs are separated from each others. Fig. 5h simplifies graphically the intersection and calculation methodology within a single discontinuity.

231 The results of the slab No. 1 (size 40.0 cm x 20.0 cm x 1.50 cm) are given in Fig. 6. For this cutting

232 grid scenario, the optimum recovery ratio was found to be 35.7 %. For this size, the optimum

233 cutting orientation is parallel to the plane XY – slab rotation 0.0° and with a displacement of (dx

234 = -0.01 m, dy = 0.1 m, dz = -0.01 m). From Fig. 6, it can be observed that the recovery ratio varies

235 within each single orientation-rotation as well as between the six orientations-rotations.

slabs legend
- intersected slabs with full size inside the block body
- non-intersected slabs with full size inside the block body
- other slabs in the 3D cutting grid of slabs

236
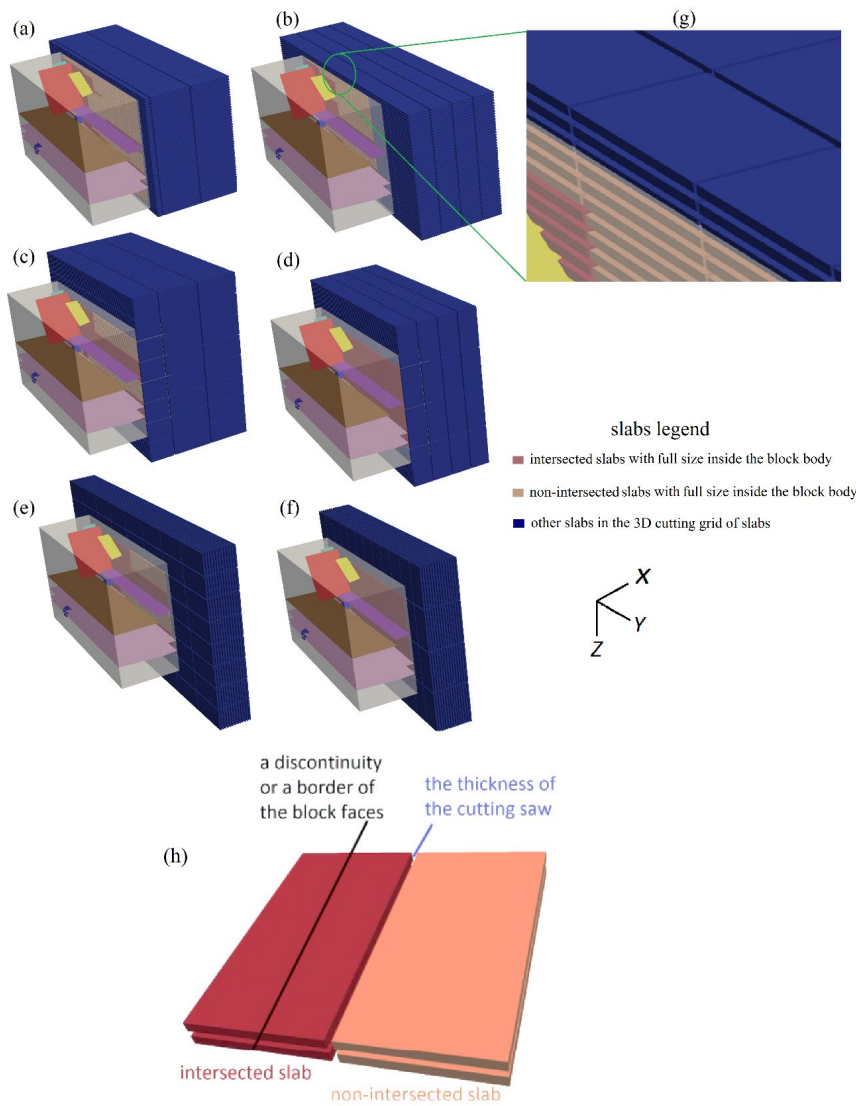
Fig. 5. The 6 orientations/rotations (sub-figures a, b, c, d, e, and f) of the cutting grid scenario using ParaView. This figure refers to the results of slab size No. 1. Details of the sub-figures a, b, c, d, e, and f are provided in Table 3. Sub-figures g and h are illustrative figures.

Table 3

The sub-figures details presented in Fig. 5.

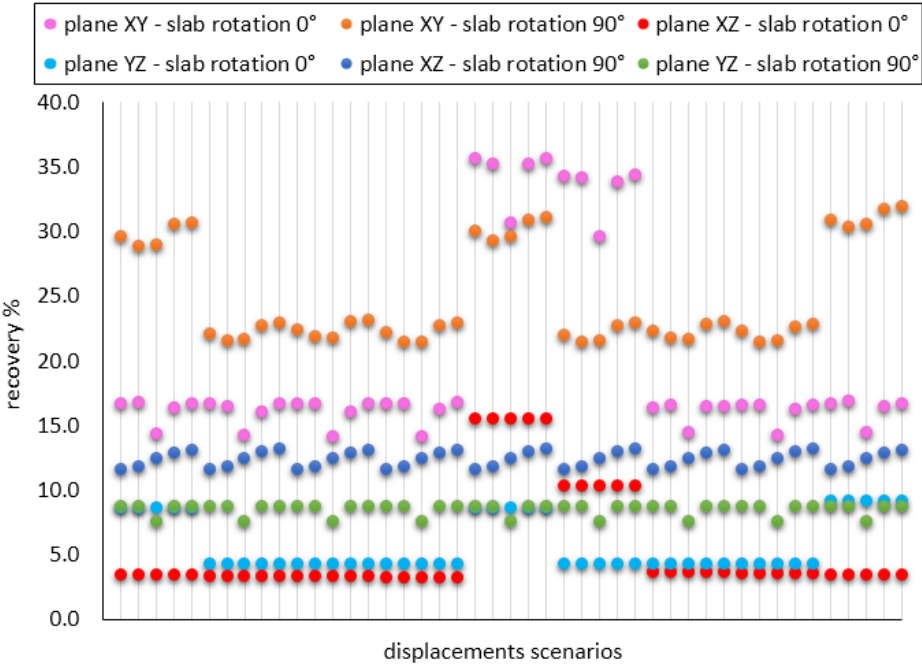| sub-figure	cutting orientation of the slabs	rotation of the slabs
Fig. 4a	XY plane	0.0°
Fig. 4b	XY plane	90.0°
Fig. 4c	XZ plane	0.0°
Fig. 4d	XZ plane	90.0°
Fig. 4e	YZ plane	0.0°
Fig. 4f	YZ plane	90.0°

Fig. 6. Graphical representation of the optimization results for the slab size No. 1.

The maximum number of non-intersected slabs and the maximum recovery ratio for each tested

slab size are represented in Fig. 7. The best recovery ratio of 44.91 % was found for the cutting

grid of the slab size No. 23. The cutting orientation is parallel to plane XY – slab rotation 90.0°,

249   with a displacement of (dx = -0.01 m, dy = 0.05 m, dz = -0.02 m), which can be taken as the most

250   environmental friendly solution. From Fig. 7, the histogram of the maximum recovery is not in

251   agreement with the maximum number of non-intersected slabs. In fact, for example, the

252   maximum recovery ratio for the slab size No. 13 is higher than for slab size No. 12. However, the

253   maximum number of non-intersected slabs for the cutting grid of slab size No. 13 is lower than

254   for slab size No. 12. This is because the volumes of slabs are different and the volume controls
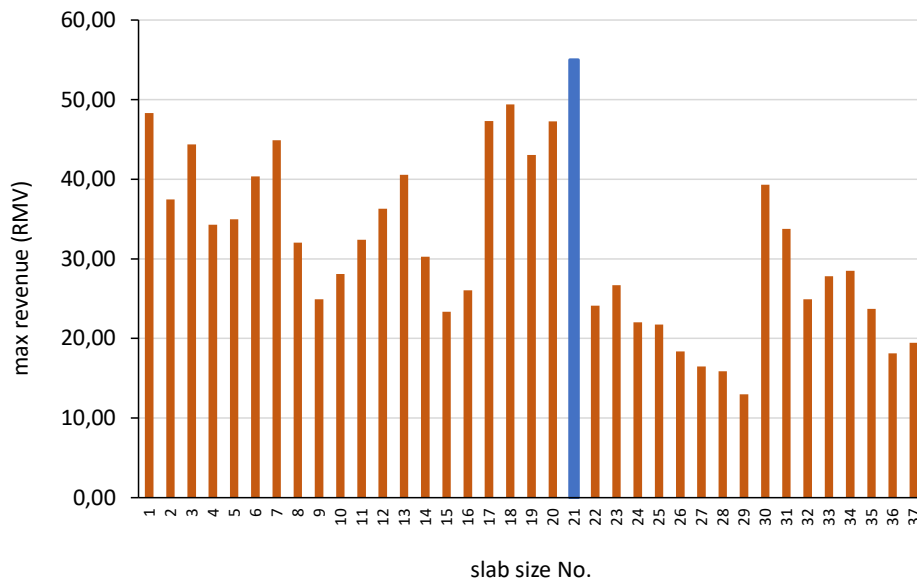
255   the recovery ratio.
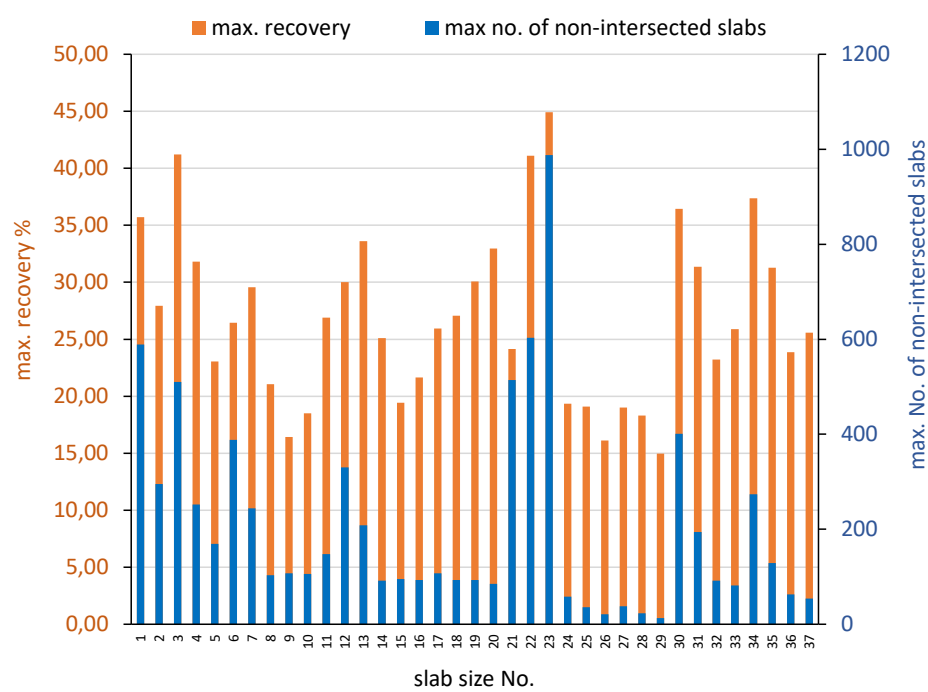
256

257   Fig. 7. Maximum recovery ratio and maximum number of non-intersected slabs for all sizes of

258   slabs .

259 From an economic point of view, neither the maximum recovery ratio nor the maximum number

260 of non-intersected slabs can be used as comparison indicator for the cutting grid optimization

261 within a range of different slab sizes. When several sizes are considered, the total revenue

262 calculated by Eq. (6) can be a more effective comparison indicator to assess the optimum

263 solution.

264 $revenue = number\ of\ non\ intersected\ slabs\ \times RMV\ per\ unit$ $\qquad\qquad$ (6)

265 Interestingly, as shown in Fig. 8, the optimal (maximum) revenue is then obtained from the

266 cutting grid scenario No. 21 with a total revenue value of 55.0 RMV. Neither the maximum

267 number of non-intersected slabs nor the maximum recovery ratio could be found in this slab size.

268 This imply that, the final economical solution (maximum RMV), given by SlabCutOpt, for this

269 block, was identified in slab size No. 21, at the cutting orientation parallel to plane XY – slab

270 rotation 0° with a displacement: (dx = -0.11 m, dy = 0.04 m, dz = -0.01), and equally at the cutting

271 orientation parallel to plane XY – slab rotation 90° with a displacement: (dx = -0.11 m, dy = 0.04

272 m, dz = -0.01). These results were expected since the slab is square-shaped (30.5 cm x 30.5 cm),

273 therefore, the slab rotation had no effect on the final results. Fig. 9 shows a 3D clip visualization

274 of the final optimal economical solution (slab size No. 21).

275

276   Fig. 8. The maximum revenue obtained for each slab size.

slabs legend

■ intersected slabs with full size inside the block body

■ non-intersected slabs with full size inside the block body
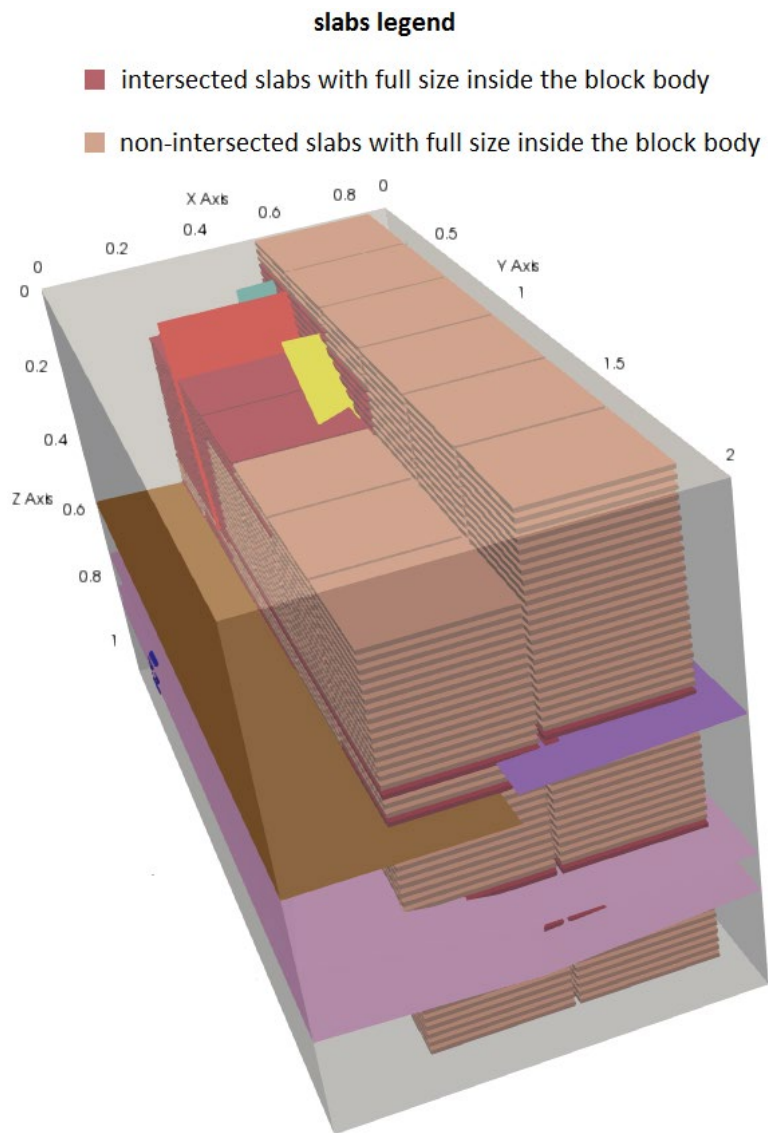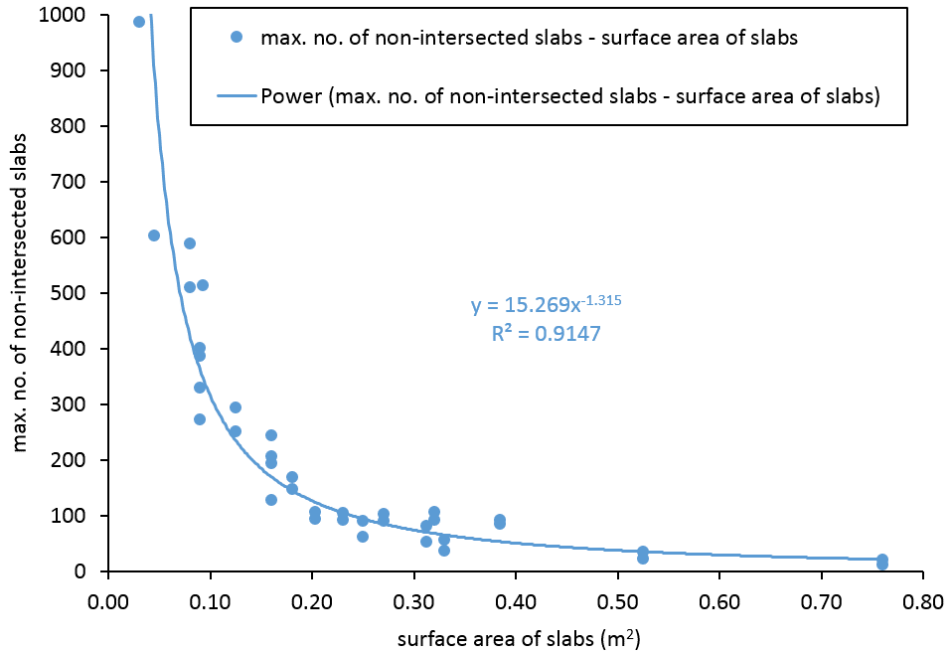
277

278   Fig. 9. A 3D clipped view of the optimal economical solution visualized using ParaView.

279   The grain texture or pattern of an ornamental stone product is an important commercial

280   characteristic. The final product aesthetic pleasure is taken in account when the block is cut for

281   applications of prestigious and decoration purposes. The rotation of the cutting grid may cause

282   a change of the final texture of the ornamental stone product in case of stones with veins or color

283   gradation patterns. The presented algorithm can be used for stones which have a uniform color

284   with a texture that is insensitive to the grid rotation and for materials used for building and

285   construction applications that do not concern with texture. It was referred to such these cases of

286   possible rotation of the cutting pattern also by [43]. If the commercial value of the slabs is known

287   (or can be estimated) for different cutting orientation/rotation, then it is still possible to estimate

288   the total revenue for each cutting grid scenario.

289   The surface area of the slabs tested, in the case study, played a main role in the run of SlabCutOpt

290   software. The maximum number of non-intersected slabs, is strongly correlated in a negative

291   power relation with the surface area value of the slabs (Fig. 10). When information about the

292   commercial price for other non-tested slab sizes in SlabCutOpt is available, the use of the

293   correlation formula (in Fig. 10) can be used to estimate their relative revenue. However,

294   SlabCutOpt will still be needed in order to know the relative geometric design of the optimum

295   cutting orientation-rotation of slabs.

The plot shows a scatter of data points with axes labeled "max. no. of non-intersected slabs" (y-axis, 0 to 1000) and "surface area of slabs (m²)" (x-axis, 0.00 to 0.80). The fitted equation is:

$$y = 15.269x^{-1.315}$$
$$R^2 = 0.9147$$

Legend:
- max. no. of non-intersected slabs - surface area of slabs
- Power (max. no. of non-intersected slabs - surface area of slabs)

296

Fig. 10. The relation between the surface area of slabs and the number of non-intersected slabs obtained for each size.

The computation time of the SlabOptCut run (considering parameter write_vtu=1, see Appendix A), on a personal computer equipped with a 64-bit operative system Windows 10, a processor Intel i7-3770K CPU @ 3.5 GHz , and an installed memory (RAM) of 8.00 GB, was 23.0 minutes. Depending by the kind of application, the computation time strongly depends on Input/Output files operations. Avoiding time consuming operation of printing out vtu files for each simulated cutting grid, the computation time was reduced up to to 37.0 seconds (considering parameter write_vtu=2, see Appendix A). The SlabCutOpt algorithm used the OpenMP[52] library to

306   compute the number of no-intersected slab for different scenarios simultaneously using several

307   threads for fast computation.

308   **5. Conclusions**

309   Cutting scenarios (3D cutting grid patterns) of a stone block could be tested using the presented

310   software code SlabCutOpt to optimize the recovery ratio or the revenue of the block. We

311   developed a 3D optimization algorithm to simulate several 3D cutting scenarios of slabs.

312   Discontinuities need to be modeled for the whole volume of the ornamental stone block. For

313   each 3D cutting scenario, the algorithm calculates the number of non-intersected slabs - with

314   discontinuities or the block body borders - which allowed calculating the recovery ratio. The

315   optimization algorithm SlabCutOpt was successfully coded in C++ and allowed to visualize the

316   optimized result in 3D using a data visualization software package, such as ParaView.

317   The presented algorithm can work with discontinuities data described in PLY files whatever the

318   detection method is. In the presented case study, the results was based on modeling

319   discontinuities, as 3D surfaces, detected by GPR survey, as recommended by the authors.

320   However, the obtained results are subjected to the limitations of the GPR method. If a tinny

321   hidden fracture could not be detected, it may lead to have unconsidered fractured slab,

322   particularly when it is open fracture. Therefore, using more than a method for fracture detection

323   or more than one GPR frequency (higher) can increase the accuracy of the discontinuities model.

324   For the presented case study of a limestone block, among 37 several -sizes of slabs, the cutting

325   grid of slab size No. 23 of dimensions 30.0 cm x 10.0 cm x 3.0 cm provided the optimum

326   production recovery ratio. Furthermore, economic factors have to be taken into account to

327   correctly evaluate the optimal solution of the cutting grid scenario. Slab size No. 21 of dimensions

328   30.5 cm x 30.5 cm x 1.0 cm provided the final optimal economical solution.

329   A negative power correlation was found between the maximum number of the non-intersected

330   slabs and the surface area of slabs. This correlation can be used, for example, to estimate the

331   maximum number of non-intersected slabs for other cutting grid sizes.

332   SlabCutOpt is recommended to be used in quarrying companies to maximize recovery and

333   revenue, it can provide stone processing factories with the slab sizes optimize the revenue and

334   minimize the waste. Moreover, SlabCutOtp allows quarrying companies to study the potential

335   revenue value of various slab sizes products enabling quarrying companies to estimate the

336   revenue and recovery when commitment with customers exists regarding certain slab sizes.

337   Waste material quantity and size can be estimated using SlabCutOpt allowing further studying of

338   waste re-processing and recycling potential.

339   Future works include the considerations of the cutting cost, energy consumption, and material

340   texture preference in the algorithm. A comparison study between the computed cutting patterns

341   by SlabCutOpt and the actual cutting results of a stone block at a processing plant is

342   recommended. A combination of non-destructive fracture detection and modeling techniques

343   and SlabCutOpt is recommended for environmental and economic sustainable reasons.

344   **Acknowledgements**

351   **References**

352   [1]   C. Montani, Stone 2002—world marketing handbook, Gruppo Editoriale Faenza Editice.,

353   Faenza, Italy, 2003.

354   [2]   C. Montani, Stone 2008—world marketing handbook., Faenza, Gruppo Editoriale Faenza

355   Editice, Faenza, 2008.

356   [3]   J. Carvalho, C. Lopes, A. Mateus, L. Martins, M. Goulão, Planning the future exploitation of

357   ornamental stones in Portugal using a weighed multi-dimensional approach, Resour.

358   Policy. 59 (2018) 298–317. doi:10.1016/j.resourpol.2018.08.001.

359   [4]   N. Careddu, Dimension stones in the circular economy world, Resour. Policy. 60 (2019)

360   243–245. doi:10.1016/j.resourpol.2019.01.012.

361   [5]   D. Macedo, R. Mori, A. Maria, P. Mizusaki, Sustainability strategies for dimension stones

362   industry based on Northwest region of Espírito Santo State , Brazil, Resour. Policy. 52

363   (2017) 207–216. doi:10.1016/j.resourpol.2017.03.005.

364   [6]   N. Careddu, G. Siotto, R. Siotto, C. Tilocca, From land fi ll to water, land and life : The

365   creation of the Centre for stone materials aimed at secondary processing, Resour. Policy.

366   38 (2013) 258–265. doi:10.1016/j.resourpol.2013.05.001.

367   [7]   N. Careddu, G. Siotto, Promoting ecological sustainable planning for natural stone

368   quarrying . The case of the Orosei Marble Producing Area in Eastern Sardinia, Resour.

369   Policy. 36 (2011) 304–314. doi:10.1016/j.resourpol.2011.07.002.

370   [8]   M. Galetakis, G. Alevizos, K. Leventakis, Evaluation of fine limestone quarry by-products,

371   for the production of building elements - An experimental approach, Constr. Build. Mater.

372   26 (2012) 122–130. doi:10.1016/j.conbuildmat.2011.05.011.

373   [9]   M. Galetakis, A. Soultana, A review on the utilisation of quarry and ornamental stone

374   industry fine by-products in the construction sector, Constr. Build. Mater. J. 102 (2016)

375   769–781. doi:10.1016/j.conbuildmat.2015.10.204.

376   [10] G. Marras, N. Careddu, Sustainable reuse of marble sludge in tyre mixtures, Resour. Policy.

377   59 (2018) 77–84. doi:10.1016/j.resourpol.2017.11.009.

378   [11] A. Cavallo, Serpentinitic waste materials from the dimension stone industry :

379   Characterization, possible reuses and critical issues, Resour. Policy. 59 (2018) 17–23.

380   doi:10.1016/j.resourpol.2018.08.003.

381   [12] D. Tumac, A. Shaterpour-Mamaghani, Estimating the sawability of large diameter circular

382   saws based on classification of natural stone types according to the geological origin, Int.

383   J. Rock Mech. Min. Sci. 101 (2018) 18–32. doi:10.1016/j.ijrmms.2017.11.014.

384   [13] M. Yurdakul, K. Gopalakrishnan, H. Akdas, Prediction of specific cutting energy in natural

385   stone cutting processes using the neuro-fuzzy methodology, Int. J. Rock Mech. Min. Sci. 67

386   (2014) 127–135. doi:10.1016/j.ijrmms.2014.01.015.

387   [14] A. Aryafar, R. Mikaeil, S. Shaffiee, S. Shaffiee, Utilization of soft computing for evaluating

388   the performance of stone sawing machines , Iranian quarries, Int. J. Min. Geo-Engineering.

389   in press (2018). doi:10.22059/IJMGE.2017.233493.594673.

390   [15]   J.F. Carvalho, P. Henriques, P. Falé, G. Luís, Decision criteria for the exploration of

391   ornamental-stone deposits: Application to the marbles of the Portuguese Estremoz

392   Anticline, Int. J. Rock Mech. Min. Sci. 45 (2008) 1306–1319.

393   doi:10.1016/j.ijrmms.2008.01.005.

394   [16]   M. Elkarmoty, C. Colla, E. Gabrielli, S. Bonduà, R. Bruno, A combination of GPR survey and

395   laboratory rock tests for evaluating an ornamental stone deposit in a quarry bench,

396   Procedia Eng. 191 (2017) 999–1007. doi:10.1016/j.proeng.2017.05.272.

397   [17]   M. Elkarmoty, C. Colla, E. Gabrielli, S. Bonduà, R. Bruno, Deterministic three-dimensional

398   rock mass fracture modeling from geo-radar survey: a case study in a sandstone quarry in

399   Italy, Environ. Eng. Geosci. 23 (2017) 314–331. doi:10.2113/gseegeosci.23.4.314.

400   [18]   M. Elkarmoty, C. Colla, E. Gabrielli, S. Kasmaeeyazdi, F. Tinti, S. Bonduà, R. Bruno, Mapping

401   and modelling fractures using ground penetrating radar for ornamental stone assessment

402   and recovery optimization: Two case studies, Mining-Geological-Petroleum Eng. Bull. 32

403   (2017) 63–76. doi:10.17794/rgn.2017.4.7.

404   [19]   J. Martínez, V. Montiel, J. Rey, F. Cañadas, P. Vera, Utilization of Integrated Geophysical

405   Techniques to Delineate the Extraction of Mining Bench of Ornamental Rocks (Marble),

406   Remote Sens. 9 (2017) 1322. doi:10.3390/rs9121322.

407   [20]   M. Elkarmoty, F. Tinti, S. Kasmaeeyazdi, F. Giannino, S. Bonduà, R. Bruno, Implementation

408   of a fracture modeling strategy based on georadar survey in a large area of limestone

409   quarry bench, Geosciences. 8 (2018) 1–15. doi:10.3390/geosciences8120481.

410   [21]   S.J. Seol, J.-H. Kim, Y. Song, S.-H. Chung, Finding the strike direction of fractures using GPR,

411   Geophys. Prospect. 49 (2001) 300–308. doi:10.1046/j.1365-2478.2001.00262.x.

412   [22]   H. Luodes, H. Sutinen, P. Härmä, H. Pirinen, O. Selonen, Assessment of potential natural

413   stone deposits, in: L.F. Lollino G., Manconi A., Guzzetti F., Culshaw M., Bobrowsky P. (Ed.),

414   Eng. Geol. Soc. Territ. - Vol. 5, Springer, Cham, 2015: pp. 243–246. doi:10.1007/978-3-319-

415   09048-1_47.

416   [23]   H. Luodes, H. Sutinen, Evaluation and modelling of natural stone rock quality using Ground

417   Penetrating Radar (GPR), in: Nenonen, K., Nurmi P.A. (Eds.), Geosci. Soc. 125th Anniv. Vol.

418   Geol. Surv. Finland, Spec. Pap. 49, 2011: pp. 83–90.

419   [24]   J. Rey, J. Martínez, P. Vera, N. Ruiz, F. Cañadas, V. Montiel, Ground-penetrating radar

420   method used for the characterisation of ornamental stone quarries, Constr. Build. Mater.

421   77 (2015) 439–447. doi:10.1016/j.conbuildmat.2014.12.076.

422   [25]   M. Lualdi, L. Zanzi, 2D and 3D experiments to explore the potential benefit of GPR

423   investigations in planning the mining activity of a limestone quarry, in: Tenth Int. Conf. Gr.

424   Penetrating Radar, GPR2004, 2004: pp. 613–616.

425   [26]   B. Koster, F. Kruse, The use of ground penetrating radar (GPR) in the investigation of

426   historical quarry abandonment in Svalbard, Polar Rec. (Gr. Brit). 52 (2016) 330–344.

427   doi:10.1017/S0032247415000844.

428   [27]   M. Grasmueck, R. Weger, H. Horstmeyer, Three-dimensional ground-penetrating radar

429   imaging of sedimentary structures, fractures, and archaeological features at submeter

430   resolution, Geology. 32 (2004) 933. doi:10.1130/G20776.1.

431   [28]   M. Yi, J. Kim, S. Cho, M. Sato, Integrated application of borehole radar reflection and

432   resistivity tomography to delineate fractures in granite quarry mine, in: Tenth Int. Conf.

433   Gr. Penetrating Radar, 21-24 June, Delft, The Netherlands, 2004: pp. 213–216.

434   [29]   L. Zanzi, A. Hojat, H. Ranjbar, S. Karimi-Nasab, A. Azadi, D. Arosio, GPR measurements to

435   detect major discontinuities at Cheshmeh-Shirdoosh limestone quarry, Iran, Bull. Eng.

436   Geol. Environ. (2017). doi:10.1007/s10064-017-1153-x.

437   [30]   D. Arosio, S. Munda, L. Zanzi, Quality control of stone blocks during quarrying activities, in:

438   14th Int. Conf. Gr. Penetrating Radar, 4-8 June 2012, Shanghai, China, 2012: pp. 822–826.

439   doi:10.1109/ICGPR.2012.6254975.

440   [31]   D. Arosio, Rock fracture characterization with GPR by means of deterministic

441   deconvolution, J. Appl. Geophys. 126 (2016) 27–34. doi:10.1016/j.jappgeo.2016.01.006.

442   [32]   M. Elkarmoty, F. Tinti, S. Kasmaeeyazdi, S. Bonduà, R. Bruno, 3D modeling of

443   discontinuities using GPR in a commercial size ornamental limestone block, Constr. Build.

444   Mater. 166 (2018) 81–86. doi:10.1016/j.conbuildmat.2018.01.091.

445   [33]   J. Rey, J. Martínez, V. Montiel, F. Cañadas, N. Ruiz, Characterization of the sedimentary

446   fabrics in ornamental rocks by using GPR, Near Surf. Geophys. 15 (2017) 457–465.

447   doi:10.3997/1873-0604.2017015.

448　[34]　A. Turanboy, A geometric approach for natural rock blocks in engineering structures,

449　　　　Comput. Geosci. 14 (2010) 565–577. doi:10.1007/s10596-009-9171-9.

450　[35]　A. Turanboy, E. Ülker, LIP-RM: An attempt at 3D visualization of in situ rock mass

451　　　　structures, Comput. Geosci. 12 (2008) 181–192. doi:10.1007/s10596-007-9077-3.

452　[36]　R. Yarahmadi, R. Bagherpour, R. Kakaie, N.H. Mirzaie, M. Yari, Development of 2D

453　　　　computer program to determine geometry of rock mass blocks, Int. J. Min. Sci. Technol.

454　　　　24 (2014) 191–194. doi:10.1016/j.ijmst.2014.01.008.

455　[37]　E. Ülker, A. Turanboy, Maximum volume cuboids for arbitrarily shaped in-situ rock blocks

456　　　　as determined by discontinuity analysis—A genetic algorithm approach, Comput. Geosci.

457　　　　35 (2009) 1470–1480. doi:10.1016/j.cageo.2008.08.017.

458　[38]　M. Mutlutürk, Determining the amount of marketable blocks of dimensional stone before

459　　　　actual extraction, J. Min. Sci. 43 (2007) 75–80. doi:10.1007/s10913-007-0008-4.

460　[39]　R. Yarahmadi, R. Bagherpour, S.G. Taherian, L.M.O. Sousa, Discontinuity modelling and

461　　　　rock block geometry identification to optimize production in dimension stone quarries,

462　　　　Eng. Geol. 232 (2018) 22–33. doi:10.1016/j.enggeo.2017.11.006.

463　[40]　M. Fernández-de Arriba, M.E. Díaz-Fernández, C. González-Nicieza, M.I. Álvarez-

464　　　　Fernández, A.E. Álvarez-Vigil, A computational algorithm for rock cutting optimisation

465　　　　from primary blocks, Comput. Geotech. 50 (2013) 29–40.

466　　　　doi:10.1016/j.compgeo.2012.11.010.

467　[41]　S. Mosch, D. Nikolayew, O. Ewiak, S. Siegesmund, Optimized extraction of dimension stone

468   blocks, Environ. Earth Sci. 63 (2011) 1911–1924. doi:10.1007/s12665-010-0825-7.

469 [42] M.M. Demarco, P. Oyhantcabal, K.-J. Stein, S. Siegesmund, Granitic dimensional stones in

470   Uruguay: evaluation and assessment of potential resources, Env. Earth Sci. 69 (2013)

471   1397–1438. doi:10.1007/s12665-012-2027-y.

472 [43] M.I. Álvarez-Fernández, C. González-Nicieza, A.E. Álvarez-Vigil, L.R. Alejano, Geometrical

473   design of ornamental stone slabs cutting using the neutral region concept, Int. J. Rock

474   Mech. Min. Sci. 52 (2012) 31–39. doi:10.1016/j.ijrmms.2012.01.012.

475 [44] P. Guigue, O. Devillers, Fast and robust triangle-triangle overlap test using orientation

476   predicates, J. Graph. Tools. 8 (2003) 25–32. doi:10.1080/10867651.2003.10487580.

477 [45] D. Vidić, I. Galić, B. Farkaš, The profitability of dimension stone deposit exploitation in

478   relation to the coefficient of utilization, Mining-Geology-Petroleum Eng. Bull. 25 (2012)

479   123–130.

480 [46] N. Careddu, G. Siotto, Promoting ecological sustainable planning for natural stone

481   quarrying. The case of the Orosei marble producing area in Eastern Sardinia, Resour.

482   Policy. 36 (2011) 304–314. doi:10.1016/j.resourpol.2011.07.002.

483 [47] G. Marras, G. Siotto, J.L. Parra, N. Careddu, Potential applications of waste material

484   deriving from marble processing plants, in: 7th Int. Marble Nat. Stones Congr. Turkey

485   (Mersem VII), 14–15 October 2010, Afyonkarahisar, Turkey, 2010: pp. 55–61.

486 [48] M. Lokeshwari, K.S. Jagadish, Eco-friendly use of granite fines waste in building blocks,

487   Procedia Environ. Sci. 35 (2016) 618–623. doi:10.1016/j.proenv.2016.07.049.

488 [49] M.E. Allam, E.S. Bakhoum, G.L. Garas, Re-use of granite sludge in producing green

489   concrete, ARPN J. Eng. Appl. Sci. 9 (2014) 2731–2737.

490 [50] Bourke P., PLY - Polygon File Format, (2011). http://paulbourke.net/dataformats/ply/

491   (accessed March 19, 2018).

492 [51] ParaView website, (n.d.). http://www.paraview.org/ (accessed May 1, 2018).

493 [52] OpenMP website, (n.d.). http://www.openmp.org/ (accessed May 1, 2018).

494

495

496

497

498

499

500

501

502 **Appendix A**

503 The directives of the working mode, the bounding domain, output options of SlabCutOpt are

504 included in the SlabCutOpt.par file. Keywords are briefly resumed in the given example file below.

```
#SlabCutOpt parameters file
# Block domain definition
x_max=+0.9 #
x_min=+0.0 #
y_max=+2.0 #
y_min=+0.0 #
z_max=+1.1 #
z_min=+0.0 #
#Cutting slab dimensions
dim_x=0.41 # Distance between cutting planes in x direction
dim_y=0.21 # Distance between cutting planes in y direction
dim_z=0.04 # Distance between cutting planes in z direction
cut_saw_thickness=0.01 # Saw thickness (meter)
#Space of solutions
#angles (radiant)
theta_step=1.570796327 #
theta_max=1.570796328 #
phi_step=1.570796327 #
phi_max=1.570796328 #
psi_step=1.570796327 #
psi_max=1.570796328 #
#displacement (meters)
dx_step=0.05 #
dy_step=0.05 #
dz_step=0.05 #
#Options
read_slab_dimensions=1 #0: read only the dimensions of the single slab indicated here;
1: consider also a list of different dimensions of slabs
read_bound=0 #0: the ply file describing the faces of the block in a form of triangles
rotation_method=1 #0: Euler rotation; 1: Cartesian axis rotation
BiDimensional=0 # #0: 3D operation; 1: 2D operation
write_vtu=1 #0: no vtu file in output; #1: for each slab size within all the tested
displacements, a slab.vtu file is generated; #2: only the solution of the maximum
number of non-intersected slabs for each slab size
read_PLY_FileList=1 #0: Read the fracture set from "test_fractures.ply"; 1 read the
PLY_FileList.dat for using several PLY files of discontinuities
end=end
```

505

506 **Appendix B**

507 The PLY file format readable by SlabCutOpt is a simplified version of the more general PLY file

508 format, such as the example below. Each element must have 3 vertices (a triangle in the 3D

509   space). The fixed characters are presented in italic, while the geometrical parameters for a

510   discontinuity description are presented in bold. After the header, a number specified in [*element*

511   *vertex*] indicates the coordinates of the vertices, then the following [*element face*] lines define

512   the number of vertices (*3*) and the vertices index of each triangle. It is worth mentioning that, in

513   the more general PLY file format, the number of vertices can be higher for polygonal elements.

```
ply
format ascii 1.0
comment example of a fracture represented by 2 triangles
element vertex 4
property float x
property float y
property float z
element face 2
property list uchar int vertex_index
end_header
0.000  2.000  0.553
0.450  2.000  0.553
0.000  0.000  0.583
0.450  0.000  0.599
3 0 1 2
3 1 2 3
```

514

515

516

517

518   **Appendix C**

519   The PLY_FileList.dat input file must contain the list of the ply files of the modelled discontinuities.

520   No header is allowed. Below is an example of PLY_FileList.dat.

block_fracturepink_g.ply
block_fracturepink_h.ply
block_fracturepink_k.ply
brown_frac.ply
extended_void_blue.ply
purple_frac.ply
red_frac.ply
single_void.ply
turquoise_frac.ply
yellow_frac.ply

521

522

523

524

525

526

527

528

529

530

531

532   **Appendix D**

533 The slab_dimensions.dat input file must contain the list of the different sizes of slabs that the

534 algorithm must test. Below is an example of slab_dimensions.dat. The order of the columns, from

535 left to right, is dim_x, dim_y, dim_z. The dimensions of the slabs must be increased by the

536 cut_saw_thickness for geometrical considerations in the algorithm.

```
0.41   0.21   0.025
0.51   0.26   0.025
0.41   0.21   0.03
0.51   0.26   0.03
0.61   0.31   0.025
0.31   0.31   0.025
0.41   0.41   0.025
0.61   0.46   0.025
0.46   0.46   0.025
0.49   0.49   0.025
0.61   0.31   0.03
0.31   0.31   0.03
0.41   0.41   0.03
0.61   0.46   0.03
0.46   0.46   0.03
0.49   0.49   0.03
```

537

538

539

540

541

542 **Appendix E**

543 The results file is an ASCII file containing the optimization results. The first part lists the dimension

544 of the slabs tested, as shown in the example below. Following, a list of solutions is provided for

545 each size. The list consists of 12 columns, from left to right there are: the order number of

546 iteration, dim_x, dim_y, dim_z, theta, phi, psi, the total number of slabs inside the block, and the

547 number of intersected slabs.

548 Optimization results:

```
Number of tested dimensions of slabs: 37

[0] dim_x= 0.410000 dim_y= 0.210000 dim_z= 0.025000
[1] dim_x= 0.510000 dim_y= 0.260000 dim_z= 0.025000
.. .. .. .. ... .. .. .. .. .. ...
[n] dim_x= 0.260000 dim_y= 1.260000 dim_z= 0.040000

Results_for_slab_[0]
..   ...   ...   ...   ...   ...   ...   ...   ...   ...   ... ...
..   ...   ...   ...   ...   ...   ...   ...   ...   ...   ... ...
..   ...   ...   ...   ...   ...   ...   ...   ...   ...   ... ...
Results_for_slab_[1]
..   ...   ...   ...   ...   ...   ...   ...   ...   ...   ... ...
..   ...   ...   ...   ...   ...   ...   ...   ...   ...   ... ...
..   ...   ...   ...   ...   ...   ...   ...   ...   ...   ... ...

764 0.510000 0.260000 0.025000 1.570796 1.570796 0.000000 -0.205000 -0.030000 -0.012500 426 121
765 0.510000 0.260000 0.025000 1.570796 1.570796 0.000000 -0.205000 0.020000 -0.012500 422 70
766 0.510000 0.260000 0.025000 1.570796 1.570796 0.000000 -0.205000 0.070000 -0.012500 422 75
767 0.510000 0.260000 0.025000 1.570796 1.570796 0.000000 -0.205000 0.120000 -0.012500 422 88
768 0.510000 0.260000 0.025000 1.570796 1.570796 0.000000 -0.155000 -0.130000 -0.012500 425 106
769 0.510000 0.260000 0.025000 1.570796 1.570796 0.000000 -0.155000 -0.080000 -0.012500 425 113

..   ...   ...   ...   ...   ...   ...   ...   ...   ...   ... ...
..   ...   ...   ...   ...   ...   ...   ...   ...   ...   ... ...
..   ...   ...   ...   ...   ...   ...   ...   ...   ...   ... ...
Results_for_slab_[n]
..   ...   ...   ...   ...   ...   ...   ...   ...   ...   ... ...
```

549